Chapter 5

Further evidence for P-wave complexity in a region with slow slip events

Note: This chapter was written in 2009 and, consequently, the locations of non-volcanic tremor and slow slip events may be out of date. The figures and text will be updated to reflect any changes in the course of preparing this chapter to be submitted for publication in the future.

5.1 Abstract

A recent study of subduction beneath central Mexico indicates that there is a relationship between the location of slow slip events (SSEs) and the location of intraslab earthquakes that generate complex P-waves. Simple P waveforms indicate normal slab conditions with no occurrences of SSEs, whereas complex P waveforms imply the presence of a thin ultra-slow velocity layer (USL) on top of the slab and the occurrence of SSEs. Here, we further test this hypothesis in a region of southwest Japan that experiences SSEs and has a dense set of local stations. We estimate the location of a possible USL along the Philippine Sea slab surface and find this region of low velocity to be coincident with locations of SSEs that have occurred in southwest Japan. We interpret the source of the possible USL layer as fluids dehydrated from the subducting plate.

5.2 Introduction

The geometry of the subducted 15–27 Ma (*Okino et al.*, 1994) Philippine Sea (PHS) plate beneath the Eurasian (EUR) plate in southwest Japan is very similar to that of the subducted 10–23 Ma (*Pardo and Suárez*, 1995; *Manea et al.*, 2004) Cocos plate beneath the North American (NAM) plate in central Mexico. Both of these young plates exhibit large lateral variations in slab dip, with segments that subduct nearly horizontally abutting segments that dip much more steeply. The PHS slab dips ∼10° towards the north beneath the island of Shikoku and ∼45° towards the west beneath the neighboring island of Kyushu (*Nakanishi*, 1980; *Zhao et al.*, 2000; *Shiomi et al.*, 2004). The Cocos slab dips ∼10–15° near the trench and then becomes subhorizontal beneath central Mexico (*Pardo and Suárez*, 1995; *Pérez-Campos et al.*, 2008). To the north, the Cocos slab dips ∼30–50°, while to the south, it dips ∼25–30° (*Pardo and Suárez*, 1995). The subduction zone in southwest Japan, however, has the added component of a second subducting plate. While the PHS plate shallowly subducts beneath the EUR plate in this region, the Pacific (PAC) plate subducts beneath the PHS plate at much greater depth (Figure 5.1).

In both the Japanese and Mexican subduction zones, SSEs have been noted to occur in the regions where the slab is dipping shallowly and where the dip of the slab is changing from nearly horizontal to a steeper dip (e.g., *Obara and Hirose*, 2006). By correlating locations of SSEs with epicenters of earthquakes that produced complex P waveforms, *Song et al.* (2009) suggested that there is a relationship between the presence of an ultra-slow velocity layer (USL) on top of the Cocos slab and location of SSEs. The locations of SSEs that have occurred in southwest Japan are shown in Figure 5.1. These episodic events are spatially and temporally correlated with the occurrence of non-volcanic tremor (NVT) in the region (*Obara et al.*, 2004; *Obara and Hirose*, 2006; *Ito et al.*, 2007). The source areas for these coincident events are estimated to occur at depths of 30 to 40 km over a 600-km-long belt parallel to the strike of the subducting PHS plate (*Obara*, 2002; *Obara and Hirose*, 2006; *Ito et al.*, 2007) (Figure 5.1). The SSEs and NVT occur in the transition zone from locked to aseismic slip in the downdip portion of the slab (*Obara and Hirose*, 2006; *Ito et al.*, 2007). These events are thought to be coupling phenomena related to stress accumulation along the upper

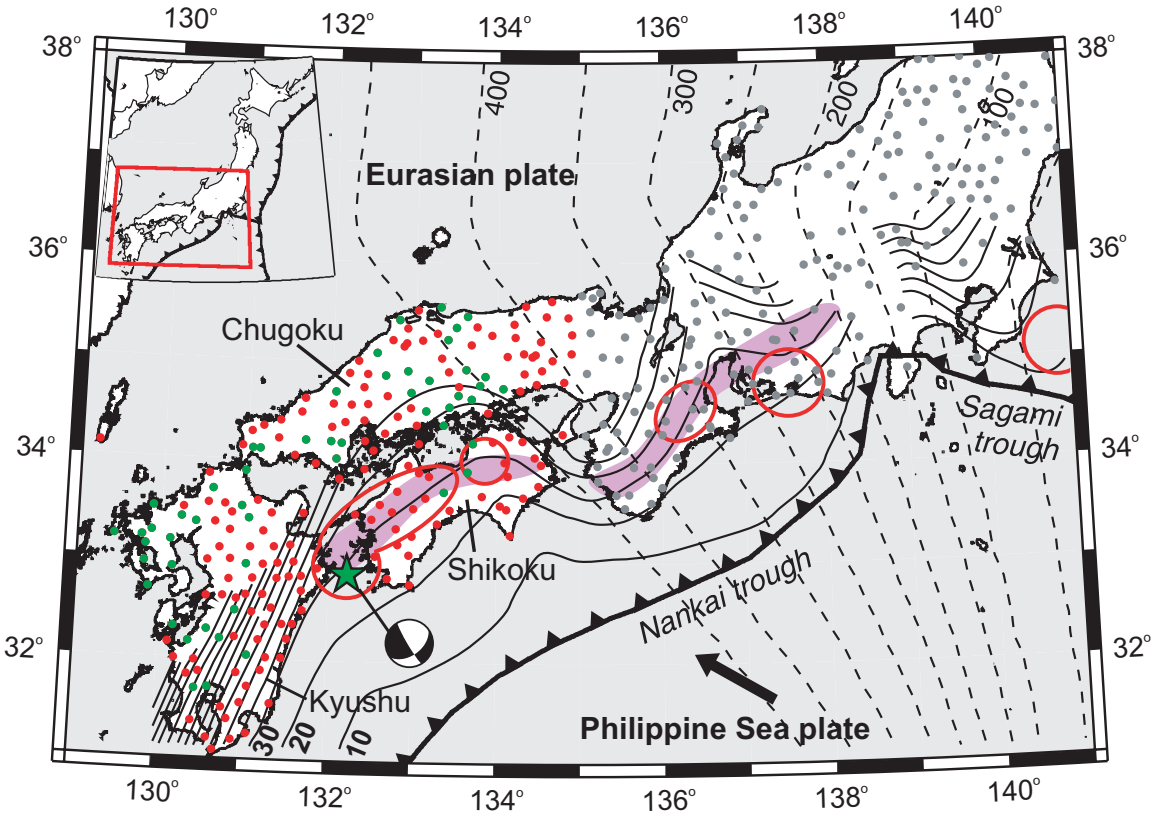

Figure 5.1: Hi-net stations in southwest Japan which recorded complex (green dots) or simple (red dots) P waveforms for the oblique-normal earthquake shown. Stations not sampled in this study are indicated by grey dots. The locations of slow slip events (red outlines) (*Hirose and Obara*, 2005; *Obara and Hirose*, 2006) and non-volcanic tremor (purple belt) (*Obara*, 2002) are indicated. The isodepth contours of the Pacific slab (*Zhao and Hasegawa*, 1993; *Nakajima and Hasegawa*, 2006) are shown by dashed lines with an interval of 50 km, while those of the Philippine Sea slab (*Wang et al.*, 2004) are shown by solid lines with an interval of 10 km. The convergence direction of the Philippine Sea plate near the Nankai trough is indicated by the black arrow (*Seno et al.*, 1993).

portion of the subducting plate, which result in an increase in the stress field updip where megathrust earthquakes occur (*Obara et al.*, 2004; *Ito et al.*, 2007). Although not completely understood, it is thought that the source of these phenomena is fluid generated by dehydration of the slab (e.g., *Obara*, 2002; *Seno and Yamasaki*, 2003; *Kodaira et al.*, 2004; *Wang et al.*, 2006). NVT could be generated by hydrofracturing during fluid migration (*Seno and Yamasaki*, 2003; *Wang et al.*, 2006; *Schwartz and Rokosky*, 2007), while at the same time, this fluid could alter the frictional properties at the slab interface, decreasing the coupling and resulting in SSEs (*Kodaira et al.*, 2004; *Obara et al.*, 2004; *Obara and Hirose*, 2006).

Several studies have provided evidence for the existence of a zone of high pore-fluid pressure along the upper boundary of the subducted PHS plate at depths of ∼25–45 km (e.g., *Honda and Nakanishi*, 2003; *Kodaira et al.*, 2004; *Wang et al.*, 2006; *Matsubara et al.*, 2009) that could cause a reduction in the effective normal stress on the plate interface, promoting SSEs. This high pore-fluid pressure zone is characterized by high-V_P/V_S (1.80–1.88) (*Matsubara et al.*, 2009), high Poisson's ratio (0.30–0.35) (*Honda and Nakanishi*, 2003; *Kodaira et al.*, 2004; *Wang et al.*, 2006), and low V_S (3.7–4.1 km/s) (*Honda and Nakanishi*, 2003; *Wang et al.*, 2006; *Matsubara et al.*, 2009). Seismic tomography reveals a region of strong low V_S, high-V_P/V_S anomaly along the top of the subducted PHS slab beneath the western Shikoku region (*Matsubara et al.*, 2009), which may indicate the presence of an USL similar to that found in central Mexico.

5.3 Data and Method

The P-wave complexities that *Song et al.* (2009) and *Song and Kim* (2012) identified as relating to the presence of an USL are locally comprised of three distinct S-to-P phases (A, B, C) that arrive within 4 sec after the P-wave (Figure 5.2). Phase A converts at the bottom of the USL and appears as a negative pulse at local stations. Phase B arrives immediately after phase A as a positive pulse, indicative of an S-to-P wave that converted at the top of the USL. Phase C converts at the base of the high velocity layer (*Dougherty et al.*, 2012; *Song and Kim*, 2012), arriving before phase A and ∼1.0–1.5 sec after the direct P-wave. At teleseismic distances, the complex P-wave of interest is

an underside reflection from the USL in which an upgoing S-wave converts to a downgoing P-wave, resulting in the phase $s_{USL}P$ (Figure 5.3). This $s_{USL}P$ phase arrives ∼3.5–4 sec after the direct P-wave.

These complex P waveforms are searched for on both local and teleseismic recordings of a selection of shallow (∼40–70 km), moderate magnitude (M5–7) intraslab earthquakes that occurred in southwest Japan between 2001 and 2003. The densely distributed Japanese Hi-net array, which is a high-sensitivity network comprised of more than 600 three-component, short-period (1 s) borehole seismometers (*Obara et al.*, 2005), is the source of the local data analyzed in this study. For teleseismic distances, data from global broadband seismometers and short-period monitoring arrays are analyzed. Each short-period monitoring array consists of a dense distribution of stations over a very small area, so the seismograms from each station within an array are stacked to produce a single record with very high signal-to-noise ratio, easing the identification of seismic phases.

5.4 Results

For the selection of earthquakes analyzed, one event had particularly good data coverage both locally and teleseismically. This M5.7 oblique-normal earthquake occurred on 25 April 2001 at a depth of 46 km in the southwest Japan region, beneath the Bungo channel (Figure 5.1) (from the Global Centroid Moment Tensor catalog (*Dziewonski et al.*, 1981; *Ekström et al.*, 2012)). Recordings of this earthquake display some complex P waveforms on local Hi-net stations (Figure 5.2) and teleseismically on individual broadband seismometers and on short-period monitoring arrays (Figure 5.3).

The locally converted S-to-P phases are visible in the complex waveforms recorded at Hi-net stations within 4 sec of the direct P-wave, while no such phases are observed in the simple waveforms (Figure 5.2). The prominence of each of the three local phases can be seen to vary with source-receiver distance and azimuth, with the strongest arrivals of all three phases occurring at stations located more than 140 km from the source in an azimuth range of ∼230°–253° (Figure 5.2). The variability of these waveforms is expected from small changes in slab geometry in this transition

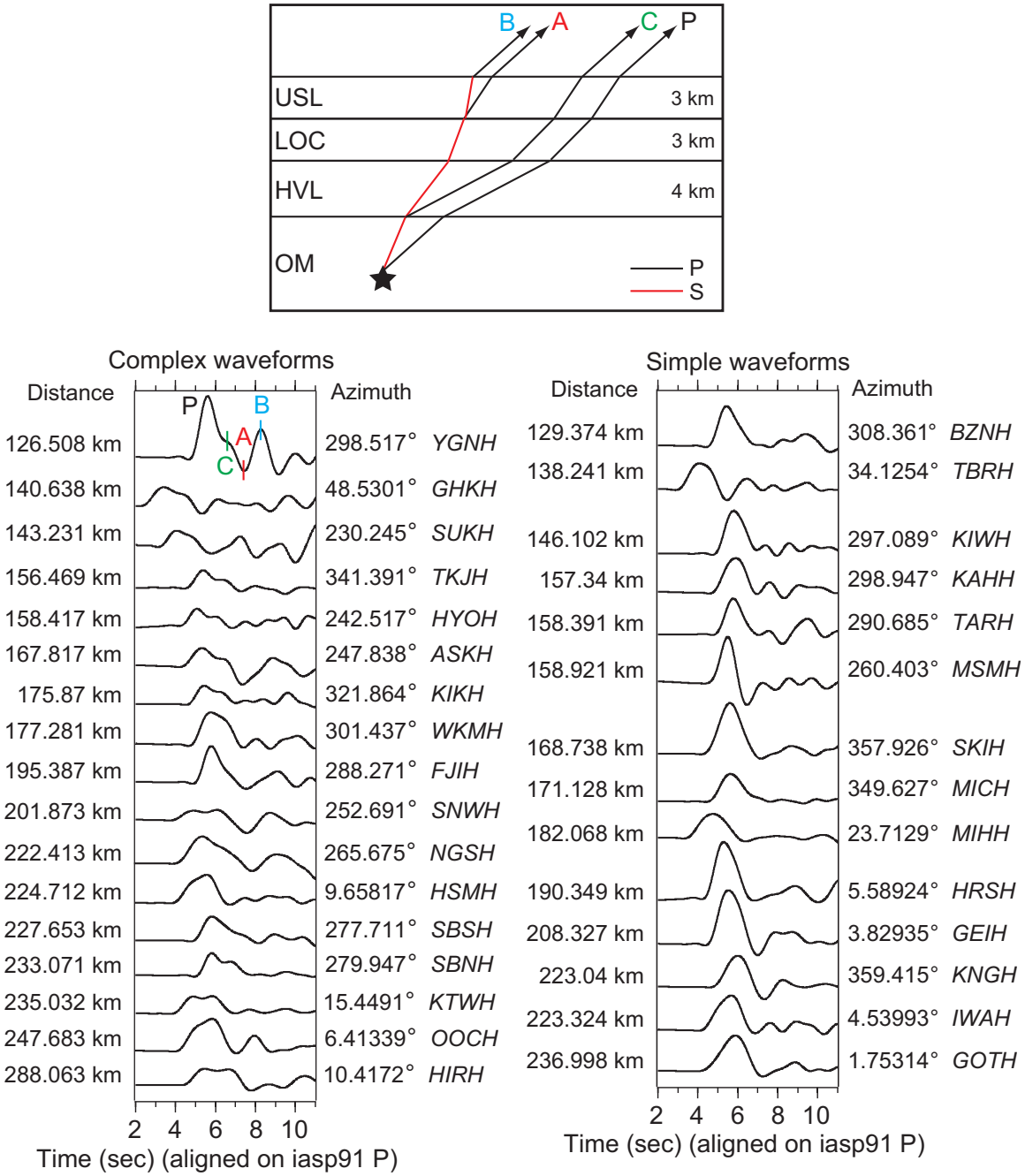

Figure 5.2: (top) Schematic cross-section illustrating the raypaths of the P-wave and the three local S-to-P phases (A, B, C) that comprise the complex P waveform. Abbreviations are USL, ultra-slow velocity layer; LOC, lower oceanic crust; HVL, high velocity layer; OM, oceanic mantle. Approximate layer thicknesses for the USL, LOC, and HVL are indicated. Modified from *Dougherty et al.* (2012). (bottom) Examples of (left) complex and (right) simple P waveforms recorded on the vertical component by the Hi-net array and filtered to 1–30 sec. S-to-P phases A, B, and C are indicated by red, blue, and green tick marks, respectively, on a single waveform as an example. The locally converted S-to-P phases are visible in the complex waveforms within 4 sec of the direct P-wave, while no such phases are observed in the simple waveforms. Station names are shown in italics.

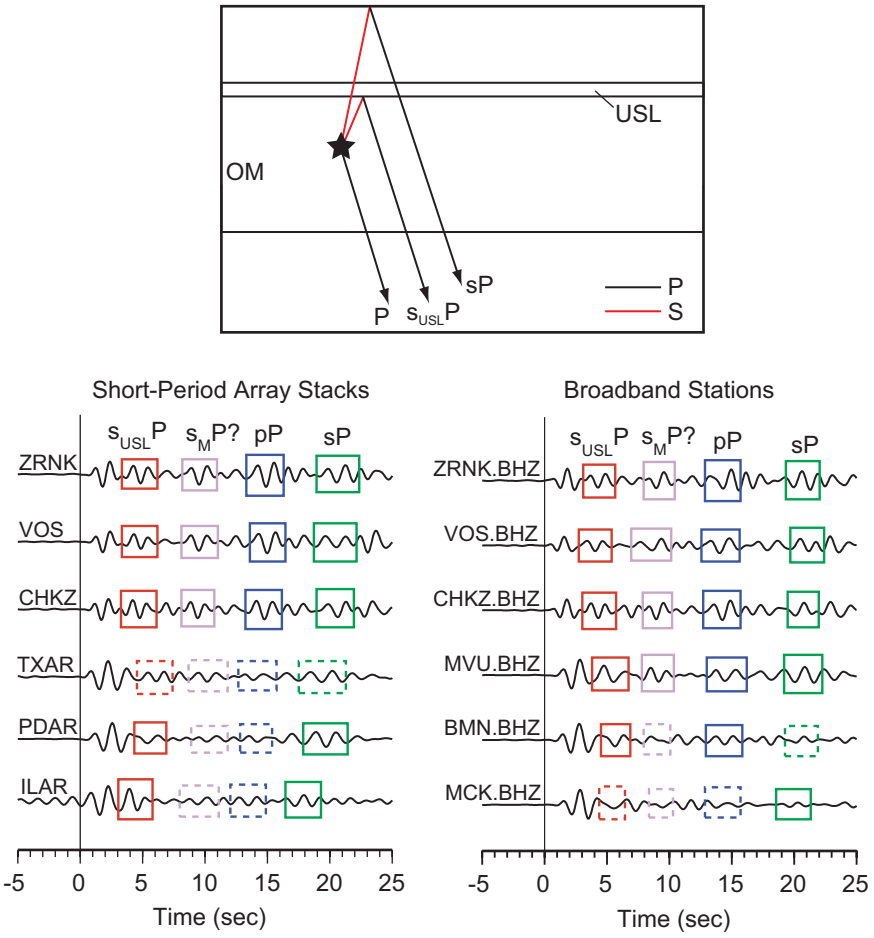

Figure 5.3: (top) Schematic diagram illustrating the raypaths of the teleseismic P-wave, the depth phase sP, and the underside reflection $s_{USL}P$ from the USL. Abbreviations are as in Figure 5.2. (bottom) Teleseismic records from (left) stacking data at six short-period arrays and from (right) broadband stations located in the vicinity of the arrays, filtered to 0.5–1 Hz. Array and station names are indicated. The arrival of the $s_{USL}P$ phase (red box) ∼3.5–4 sec after the direct P-wave is indicated. The arrivals of the depth phases pP (blue box) and sP (green box), along with a possible underside reflection from the Moho of the overriding plate (s_MP; purple box) are also shown. Possible arrivals that are not distinct are indicated by dashed boundaries. The locations of the short-period arrays and broadband stations are shown in Figure 5.4.

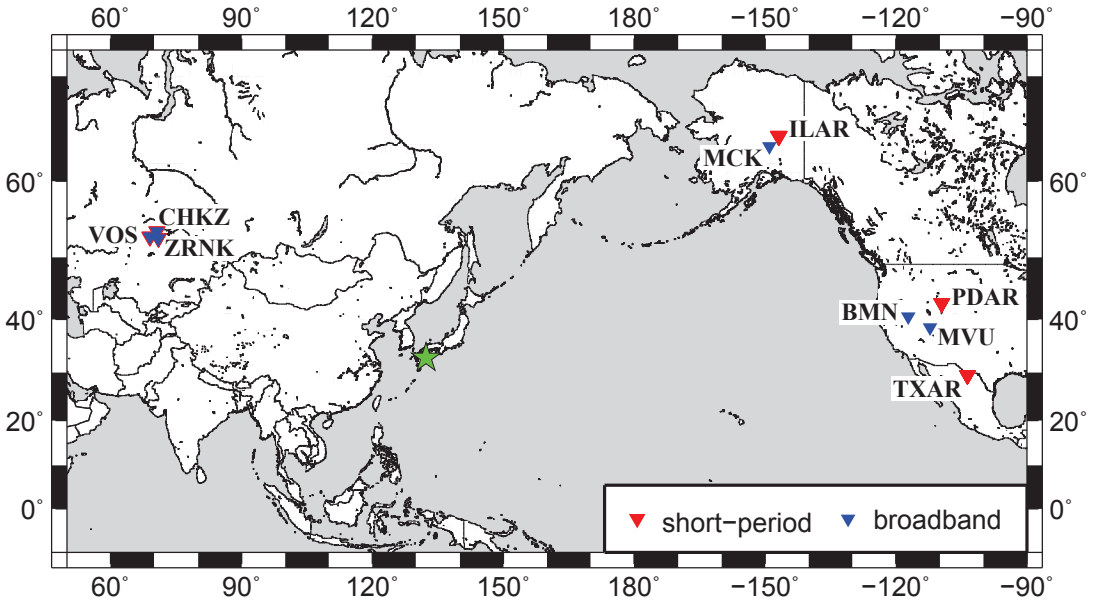

Figure 5.4: Map showing the locations of the short-period arrays (red inverted triangles) and broadband stations (blue inverted triangles) used in this study. Array and station names are indicated. For the CHKZ, ZRNK, and VOS arrays, note that the corresponding broadband stations are co-located and have the same name (see Figure 5.3). The event location is indicated by the green star.

region from subhorizontal to normal subduction.

The teleseismic underside reflection $s_{USL}P$ is clearly identifiable in five of six short-period array stacks presented in Figure 5.3; data from the sixth array indicates a possible $s_{USL}P$ phase that is not easily distinguished. Observations of this phase on broadband stations located in the vicinity of these short-period arrays (Figures 5.3 and 5.4) demonstrate that the appearance of this phase is not limited to short-period instruments. Consistent with the estimation of *Song et al.* (2009), this $s_{USL}P$ phase arrives ∼3.5–4 sec after the direct P-wave in both the short-period and broadband data at these teleseismic distances.

The locations of the S-to-P conversion points and underside reflection bounce points at the top of the PHS slab are estimated using the TauP Toolkit (*Crotwell et al.*, 1999) with the iasp91 velocity model (*Kennett and Engdahl*, 1991). A possible region for the USL is proposed based on the locations of conversion points for Hi-net stations that recorded complex and simple P waveforms and bounce points for teleseismic short-period arrays and broadband stations that recorded the

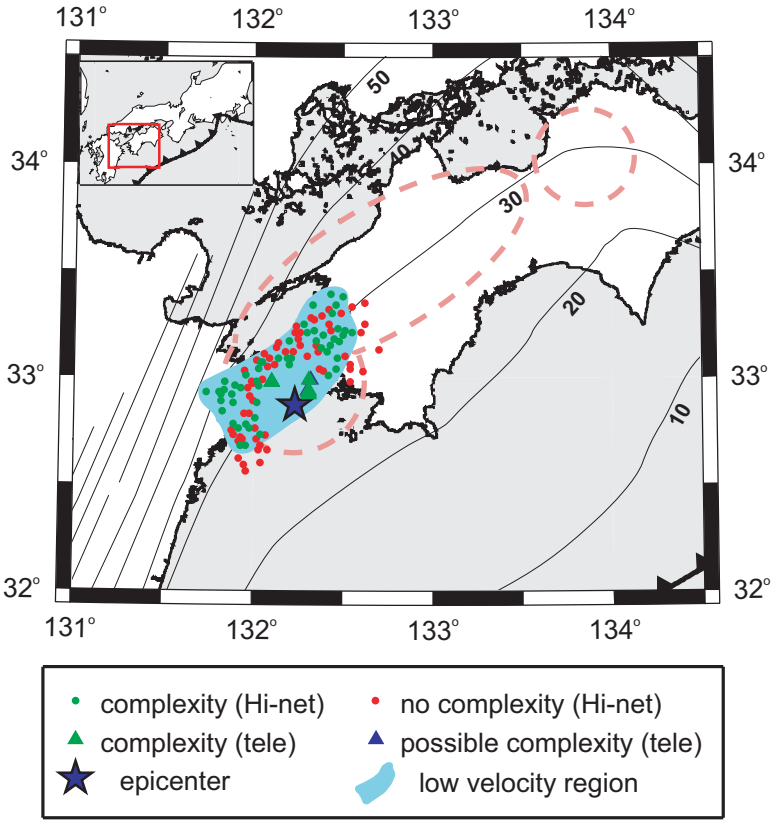

Figure 5.5: Local S-to-P conversion points and underside reflection bounce points from the top of the Philippine Sea slab for Hi-net stations that recorded complex (green dots) and simple (red dots) P waveforms and for teleseismic short-period arrays and broadband stations that recorded the $s_{USL}P$ phase (triangles), respectively. Bounce points for $s_{USL}P$ arrivals that are not distinct are indicated by blue triangles. A possible region for the USL (light blue) is proposed based on the locations of these conversion and bounce points. The locations of slow slip events (pink dashed outlines) and the Philippine Sea slab isodepth contours (thin black lines) are as in Figure 5.1.

$s_{USL}P$ phase (Figure 5.5). The intermingling of S-to-P conversion points for stations that recorded complex P waveforms and those that recorded simple P waveforms indicates that the proposed USL in southwest Japan is likely laterally heterogeneous, consistent with the observations of *Song et al.* (2009) for central Mexico.

5.5 Discussion and Conclusions

Observations of complex P waveforms both locally and teleseismically for an intraslab earthquake that occurred in a region of southwest Japan known to produce SSEs provides further evidence

for the proposed relationship between the location of SSEs and the presence of an USL on top of the slab. Using the locations of S-to-P conversion points and underside reflection bounce points at the top of the PHS slab for complex P waveforms, we are able to estimate the location of a possible USL along the slab surface. This region of very low velocity is spatially coincident with locations of SSEs that have occurred in southwest Japan and may represent part of the subducted oceanic crust that is fluid-saturated, forming a high pore-fluid pressure layer (*Song et al.*, 2009). This layer would be expected to greatly reduce the effective normal stress on the plate interface, decreasing the coupling, and promoting SSEs. The source of this fluid is thought to be dehydration of hydrous minerals in the subducted oceanic crust. A low permeability layer consisting of fine-grained blueschist located directly above the high pore-fluid pressure layer is proposed to seal in the fluid (*Song et al.*, 2009). Lateral variations in the amount of fluid released from the slab could produce the laterally heterogeneous structure of the proposed USL. This is consistent with the undulating variation from thicker, more hydrated regions to thinner, less hydrated regions that was modeled for the low velocity layer on top of the Tonga-Fiji slab (*Savage*, 2012). Alternatively, the proposed USL may occur in isolated patches of variable size, similar to the asperity model of stress distribution on the fault plane (*Lay et al.*, 1982; *Bilek and Lay*, 2002). Waveform modeling of such an asperity-like structure for the USL could provide further insights into its heterogeneity.

A seismic explosion survey conducted by *Ueno et al.* (2009) in the Tokai region of southwest Japan used wide-angle seismic reflections and 2D forward modeling by the finite-difference method to show the existence of a thin (∼2–3 km) low velocity (V_P∼4 km/s) layer in the upper part of the PHS slab. Their model results suggest that SSEs occur within this layer. Regional variations in the strength of reflections from this layer imply that it is laterally heterogeneous (*Ueno et al.*, 2009), consistent with our observations. Further fine-scale seismic modeling of the subduction zone in southwest Japan is needed in order to provide constraints on the thickness and velocity of the possible USL at the top of the PHS slab.

The spatial correlation of locations of SSEs in both southwest Japan and central Mexico with regions where the subducted plate is dipping shallowly may be related to the geometry of the plate

itself. When the slab is subducting at a very low angle and nearly underplating the overriding plate at a shallow depth, the fine-grained blueschist cap layer which creates a low permeability barrier for the fluid-saturated USL below (*Song et al.*, 2009) may exist for a long distance perpendicular to the trench. Thus, the fluid released by dehydration of the subducted oceanic crust may disperse and/or become trapped along the slab surface over a broad region, creating a high pore-fluid pressure zone in which SSEs could occur. This is contrary to the case of a more steeply subducting slab in which fluid is released at depths beyond the stability field of blueschist (e.g., *Hacker et al.*, 2003), effectively preventing the formation of a high pore-fluid pressure layer due to the lack of a low permeability seal.

5.6 Future Work

Waveform modeling of the fine-scale seismic structure of the subduction zone in southwest Japan using a 2D finite-difference algorithm can be performed in order to provide constraints on the thickness, velocity, and lateral extent of the possible USL atop the PHS slab. Additional modeling of the potential asperity-like structure proposed for the USL will explore the nature of its observed lateral heterogeneity. This study can further be strengthened through the analysis of more recent events which have occurred in this region.

References

Bilek, S., and T. Lay (2002), Tsunami earthquakes possibly widespread manifestations of frictional conditional stability, *Geophys. Res. Lett.*, *29*, 1673, doi:10.1029/2002GL015215.

Crotwell, H. P., T. J. Owens, and J. Ritsema (1999), The TauP Toolkit: Flexible seismic travel-time and ray-path utilities, *Seis. Res. Lett.*, *70*(2), 154–160.

Dougherty, S. L., R. W. Clayton, and D. V. Helmberger (2012), Seismic structure in central Mexico: Implications for fragmentation of the subducted Cocos plate, *J. Geophys. Res.*, *117*, B09316, doi:10.1029/2012JB009528.

Dziewonski, A. M., T.-A. Chou, and J. H. Woodhouse (1981), Determination of earthquake source parameters from waveform data for studies of global and regional seismicity, *J. Geophys. Res.*, *86*, 2825–2852, doi:10.1029/JB086iB04p02825.

Ekström, G., M. Nettles, and A. M. Dziewonski (2012), The global CMT project 2004-2010: Centroid-moment tensors for 13,017 earthquakes, *Phys. Earth Planet. Inter.*, *200-201*, 1–9, doi: 10.1016/j.pepi.2012.04.002.

Hacker, B. R., G. A. Abers, and S. M. Peacock (2003), Subduction factory, 1, Theoretical mineralogy, densities, seismic wave speeds, and H_2O contents, *J. Geophys. Res.*, *108*, 2029, doi: 10.1029/2001JB001127.

Hirose, H., and K. Obara (2005), Repeating short- and long-term slow slip events with deep tremor activity around the Bungo channel region, southwest Japan, *Earth Planets Space*, *57*, 961–972.

Honda, S., and I. Nakanishi (2003), Seismic tomography of the uppermost mantle beneath southwestern Japan: Seismological constraints on modelling subduction and magmatism for the Philippine Sea slab, *Earth Planets Space*, *55*, 443–462.

Ito, Y., K. Obara, K. Shiomi, S. Sekine, and H. Hirose (2007), Slow earthquakes coincident with episodic tremors and slow slip events, *Science*, *315*, 503–506.

Kennett, B. L. N., and E. R. Engdahl (1991), Travel times for global earthquake location and phase association, *Geophys. J. Int.*, *105*, 429–465.

Kodaira, S., T. Iidaka, A. Kato, J. Park, T. Iwasaki, and Y. Kaneda (2004), High pore fluid pressure may cause silent slip in the Nankai Trough, *Science*, *304*, 1295–1298.

Lay, T., H. Kanamori, and L. Ruff (1982), The asperity model and the nature of large subduction zone earthquakes, *Earthquake Pred. Res.*, *1*, 3–71.

Manea, V. C., M. Manea, V. Kostoglodov, C. A. Currie, and G. Sewell (2004), Thermal structure, coupling and metamorphism in the Mexican subduction zone beneath Guerrero, *Geophys. J. Int.*, *158*, 775–784.

Matsubara, M., K. Obara, and K. Kasahara (2009), High-V_P/V_S zone accompanying non-volcanic tremors and slow-slip events beneath southwestern Japan, *Tectonophysics*, *472*, 6–17, doi: 10.1016/j.tecto.2008.06.013.

Nakajima, J., and A. Hasegawa (2006), Anomalous low-velocity zone and linear alignment of seismicity along it in the subducted pacific slab beneath Kanto, Japan: Reactivation of subducted fracture zone?, *Geophys. Res. Lett.*, *33*, L16309, doi:10.1029/2006GL026773.

Nakanishi, I. (1980), Precursors to ScS phases and dipping interface in the upper mantle beneath southwestern Japan, *Tectonophysics*, *69*, 1–35.

Obara, K. (2002), Nonvolcanic deep tremor associated with subduction in southwest Japan, *Science*, *296*, 1679–1681.

Obara, K., and H. Hirose (2006), Non-volcanic deep low-frequency tremors accompanying slow slips in the southwest Japan subduction zone, *Tectonophysics*, *417*, 33–51.

Obara, K., H. Hirose, F. Yamamizu, and K. Kasahara (2004), Episodic slow slip events accompanied by non-volcanic tremors in southwest Japan subduction zone, *Geophys. Res. Lett.*, *31*, L23602, doi:10.1029/2004GL020848.

Obara, K., K. Kasahara, S. Hori, and Y. Okada (2005), A densely distributed high-sensitivity seismograph network in Japan: Hi-net by National Research Institute for Earth Science and Disaster Prevention, *Review of Scientific Instruments*, *76*, 021301, doi:10.1063/1.1854197.

Okino, K., Y. Shimakawa, and S. Nagaoka (1994), Evolution of the Shikoku Basin, *J. Geomag. Geoelec.*, *46*, 463–479.

Pardo, M., and G. Suárez (1995), Shape of the subducted Rivera and Cocos plates in southern Mexico: Seismic and tectonic implications, *J. Geophys. Res.*, *100*, 12,357–12,373.

Pérez-Campos, X., Y. Kim, A. Husker, P. M. Davis, R. W. Clayton, A. Iglesias, J. F. Pacheco, S. K. Singh, V. C. Manea, and M. Gurnis (2008), Horizontal subduction and truncation of the Cocos plate beneath central Mexico, *Geophys. Res. Lett.*, *35*, L18303, doi:10.1029/2008GL035127.

Savage, B. (2012), Seismic constraints on the water flux delivered to the deep earth by subduction, *Geology*, *40*, 235–238, doi:10.1130/G32499.1.

Schwartz, S. Y., and J. M. Rokosky (2007), Slow slip events and seismic tremor at circum-Pacific subduction zones, *Rev. Geophys.*, *45*, RG3004, doi:10.1029/2006RG000208.

Seno, T., and T. Yamasaki (2003), Low-frequency tremors, intraslab and interplate earthquakes in Southwest Japan—from a viewpoint of slab dehydration, *Geophys. Res. Lett.*, *30*(22), 2171, doi:10.1029/2003GL018349.

Seno, T., S. Stein, and A. E. Gripp (1993), A model for the motion of the Philippine Sea plate consistent with NUVEL-1 and geological data, *J. Geophys. Res.*, *98*, 17,941–17,948, doi: 10.1029/93JB00782.

Shiomi, K., H. Sato, K. Obara, and M. Ohtake (2004), Configuration of the subducting Philippine Sea plate beneath southwest Japan revealed from receiver function analysis based on the multivariate autoregressive model, *J. Geophys. Res.*, *109*, B04308, doi:10.1029/2003JB002774.

Song, T. A., and Y. Kim (2012), Anisotropic uppermost mantle in young subducted slab underplating Central Mexico, *Nature Geosci.*, *5*, 55–59, doi:10.1038/NGEO1342.

Song, T. A., D. V. Helmberger, M. R. Brudzinski, R. W. Clayton, P. Davis, X. Pérez-Campos, and S. K. Singh (2009), Subducting slab ultra-slow velocity layer coincident with silent earthquakes in southern Mexico, *Science*, *324*, 502–506.

Ueno, T., T. Takeda, K. Obara, and Y. Asano (2009), Seismic explosion survey around slow events in the Tokai region, Japan, *Eos Trans. AGU*, *90*(52), Abstract T11C–1837.

Wang, K., I. Wada, and Y. Ishikawa (2004), Stress in the subducting slab beneath southwest Japan and relation with plate geometry, tectonic forces, slab dehydration, and damaging earthquakes, *J. Geophys. Res.*, *109*, B08,304, doi:10.1029/2003JB002888.

Wang, Z., D. Zhao, O. P. Mishra, and A. Yamada (2006), Structural heterogeneity and its implications for the low frequency tremors in Southwest Japan, *Earth Planet. Sci. Lett.*, *251*, 66–78.

Zhao, D., and A. Hasegawa (1993), P-wave tomographic imaging of the crust and upper mantle beneath the Japan Islands, *J. Geophys. Res.*, *98*, 4333–4353.

Zhao, D., K. Asamori, and H. Iwamori (2000), Seismic structure and magmatism of the young Kyushu subduction zone, *Geophys. Res. Lett.*, *27*, 2057–2060.